Three-Dimensional Analysis of a Radiant Furnace-Application to Nitric Oxide Decomposition

R. W. Lyczkowski,* C. S. Wang† L. S. H. Chow,‡ T. R. Johnson,§ and G. F. Berry†
Argonne National Laboratory, Argonne, Illinois

The objectives of this investigation are to 1) analyze the three-dimensional steady-state fluid flow and temperature patterns in an experimental magnetohydrodynamics (MHD) radiant furnace; 2) use these results, together with a transient three-dimensional tracer simulation, to develop a one-dimensional temperature/flow model for characteristic residence times and temperatures; and 3) use this model to interpret experimental nitric oxide (NO) decomposition data. Calculated results from two three-dimensional thermal hydraulics computer programs indicate highly three-dimensional flow patterns. The high velocity gas stream entering the furnace from the diffuser hits the slag screen and flows downward, splitting into two characteristic flow paths: one close to the slag screen and one much further below it. The gas along these two flow paths then flows upward through the staggered tubes forming the lower section of the slag screen. The three-dimensional calculations were used to develop a one-dimensional temperature/flow model used as input to a one-dimensional chemical kinetics code. Good agreement with experimental NO concentrations has demonstrated the usefulness of the general methodology for interpreting experimental gas reaction data related to radiant furnaces, and as an aid in the design of high temperature furnaces and boilers for unconventional or severe services.

Nomenclature

C_1, C_2, C_μ = constants in k-ϵ turbulence model
C_p = heat capacity at constant pressure, kJ/(kg·K)
g_j = acceleration due to gravity in direction x_j, m/s^2
G_k = source due to thermal stratification in turbulent kinetic energy equation, kg/(m·s^3)
h = enthalphy, J/kg
k = turbulent kinetic energy, m^2/s^2
p = pressure, Pa
P_k = source due to mean shear in turbulent kinetic energy equation, kg/(m·s^3)
$\dot{Q}$ = heat source, W/m^3
R_j = distributed resistance
S_Φ = source term in differential equation
t = time, s
T = temperature, K
u_j = velocity in direction x_j, m/s
x_j = coordinate direction j, m
γ_v = volume porosity (fraction of the volume occupied by the fluid)
γ_j = surface permeability (fraction of the surface area unobstructed to fluid flow) in direction x_j
Γ_Φ = diffusion coefficient in differential equation
ϵ = turbulent kinetic energy dissipation rate, m^2/s^3
λ = thermal conductivity, W/(m·K)
λ_t = turbulent thermal conductivity, W/(m·K)
μ = laminar viscosity, Pa·s
μ_t = turbulent viscosity, Pa·s
Φ = dependent variable in differential equation
ρ = density, kg/m^3
$\sigma_h, \sigma_k, \sigma_\epsilon$ = Prandtl numbers for turbulent thermal energy transfer, turbulent kinetic energy and turbulent kinetic energy dissipation rate in k-ϵ turbulence model

Received June 25, 1985; revision submitted Feb. 27, 1986.

*Chemical Engineer, Energy and Environmental Systems Division.
†Mechanical Engineer, Energy and Environmental Systems Division.
‡Mechanical Engineer, Engineering Division.
§Chemical Engineer, Chemical Technology Division.

Introduction

UNDERSTANDING the temperature and flow profiles of furnace combustion gases is essential for the prediction of the chemical behavior of these gases, as well as for the design of high-temperature furnaces and boilers intended for unconventional or severe service. These temperature and flow profiles tend to be highly three-dimensional, and ultimately a fully three-dimensional chemical kinetics code will be required to accurately describe the furnace performance. A simpler one-dimensional temperature/flow model that yields results in acceptable agreement with experimental data is needed. Such a model is of use in interpreting experimental data on the evolution of chemical compounds in high-temperature furnaces, and it will help in analyzing the design of such furnaces. This paper presents a general methodology developed at Argonne National Laboratory (ANL) to produce such a temperature/flow model. The methodology consists of developing a one-dimensional representation of the three-dimensional flow and temperature calculations for use as input to a one-dimensional chemical kinetics code.

Work is underway in the Argonne National Laboratory MHD program to develop a practical diffuser outlet/boiler inlet design. One such concept is to install a solid water-cooled slag screen in the radiant furnace of the Department of Energy owned Coal Fired Flow Facility (CFFF) at the University of Tennessee Space Institute (UTSI). The screen located across the diffuser jet directs the gas downward to produce a more uniform flow distribution in the furnace. Several tests have been conducted by UTSI to evaluate the heat transfer and NO decomposition occurring in this experimental furnace.[1-3] To complement the UTSI activities. Argonne National Laboratory has made an independent analysis of these data, especially the data on NO decomposition.

A variety of one-dimensional engineering models exist to characterize and analyze MHD processes such as combustion. NO decomposition, slag formation and radiant heat trans-

fer.[4,5] These models require inputs and submodels, which must be tuned through data analysis. Such models may be adequate for predominantly one-dimensional flows. However, the analysis of the radiant furnace requires three-dimensional models, and no such comprehensive three-dimensional models to the authors' knowledge yet exist. The one-dimensional models will continue to be used for some time then, but they will require an increasing number of assumptions (concerning residence times, for example).

The COMMIX-1A[6] code was chosen to perform the three-dimensional thermal hydraulics computations because of its ready availability, extreme flexibility in simulating turbulent flows for complicated geometries, and capability of including coupled heat transfer calculations. The code developed at Argonne National Laboraory (ANL) under the sponsorship of the Nuclear Regulatory Commission (NRC) has been used extensively in analyzing three-dimensional, transient and steady-state, and single phase thermal hydraulics in nuclear reactor components and has been validated against a variety of experiments.[7-9]

While this code does not yet contain all the components necessary to model MHD processes (e.g., chemical reactions and radiation heat transfer), it can be used to begin to close the gap that exists between the one-dimensional engineering codes and a comprehensive three-dimensional code. In addition, it can be used to generate missing information necessary for input to one-dimensional analyses or to justify some of the key assumptions made and, ultimately, can be combined with the one-dimensional engineering code submodels, as desired. For example, chemical reaction equations may be added to calculate the local concentration of NO decomposition in the radiant furnace or jet impingement may be calculated to estimate the erosion of boiler walls.

A Brief Description of the COMMIX-1A Computer Program

In the COMMIX-1A computer program,[6] a modified, advanced version of COMMIX-1,[10] the conservation of mass, momentum, and energy equations are solved as a boundary value problem in space and an initial-value problem in time. The basic numerical scheme used is the Implicit Continuous Eulerian (ICE) method developed at Los Alamos National Laboratory.[11] This basic method has been supplemented in the most recent version of the code with an additional user-selected fully implicit numerical method.[12] Several unique features make it particularly suited for modeling fluid and thermal mixing in complex geometries. At present, Cartesian and cylindrical coordinate systems are available. All the simulations in this paper were performed using Cartesian coordinates and the fully implicit numerical method.

Turbulence is modeled using global constant input values of effective turbulent viscosity and thermal conductivity, which are added to the laminar values. The effective viscosity and thermal conductivity could be estimated using simple models.[6,10]

The conservation equations of mass, momentum, energy, turbulent kinetic energy, and turbulent kinetic energy dissipation solved possess a common form. If we denote the general dependent variable as Φ, the corresponding conservation equations in the quasicontinuum formulation have the following form (in tensor notation):

$$\underset{\text{(unsteady)}}{\frac{\partial}{\partial t}(\gamma_v \rho \Phi)} + \underset{\text{(convection)}}{\frac{\partial}{\partial x_j}(\gamma_j \rho u_j \Phi)} = \underset{\text{(diffusion)}}{\frac{\partial}{\partial x_j}\left(\gamma_j \Gamma_\Phi \frac{\partial \Phi}{\partial x_j}\right)} + \underset{\text{(source)}}{\gamma_v S_\Phi} \qquad (1)$$

The effective diffusion coefficient Γ_Φ and the source term S_Φ are specific to each meaning of Φ. These terms for all conservation equations are given in Table 1 (as are the various constants used for the k-ϵ two-equation turbulence model). Equation (1) reduces to the conservation equations for a continuum regime when we make porosities and permeabilities equal one ($\gamma_v = \gamma_j = 1.0$), distributed resistances equal zero ($R_j = 0$), and heat liberated from submerged solids equal zero.

Isothermal Flowfield Studies

This section describes the models and results of steady-state three-dimensional isothermal flowfield studies for the CFFF radiant furnance. An assessment is made concerning the sensitivity of the computed results for the following items: 1) coarse mesh vs finer mesh, 2) constant turbulent viscosity mode vs two-equation k-ϵ turbulence modeling, and 3) the detail to which the slag screen tubes need to be modeled as a porous medium.

Description of the CFFF Radiant Furnace

The CFFF radiant furnace section is square in cross-section, 1.22 m by 1.22 m (4 ft by 4 ft). The combustion gases leaving the diffuser enter the radiant furnace through a rectangular opening, 0.575 m (1.885 ft) wide and 0.613 m (2.01 ft) high, centered on the front wall of the furnace as shown in Fig. 1. Together with the slag trap, the furnace extends about 5 m (15 ft) below and over 10 m (30 ft) above the horizontal centerline of the diffuser inlet. A slag screen, which is a solid section of ceramic-coated water-cooled tubes about 3 in. (0.0762 m)

Table 1 Terms for equations in the general form of Eq. (1) and constants used in COMMIX-1A and -1B[6,13]

Equation	Φ	Γ_Φ	S_Φ
Continuity	1	0	0
Momentum	u_j	$\mu+\mu_t$	$\rho g_j - R_j - \frac{\partial p}{\partial x_j}$
Energy	h	$(\lambda+\lambda_t)/C_p$	$\frac{\partial p}{\partial t} + u_j \frac{\partial p}{\partial x_j} + \dot{Q}$
Turbulent kinetic energy	k	$\mu_t/\sigma_k + \mu$	$P_k + G_k - \rho\epsilon$
Turbulent kinetic energy dissipation rate	ϵ	$\mu_t/\sigma_\epsilon + \mu$	$C_1\epsilon(P_k+G_k)/k - C_2\rho\epsilon^2/k$

$$P_k = \mu_t\left[\frac{\partial u_i}{\partial x_j}\left(\frac{\partial u_i}{\partial x_j}+\frac{\partial u_j}{\partial x_i}\right)\right], \quad G_k = -\frac{\mu_t}{\rho\sigma_h}\frac{\partial \rho}{\partial T}\left(\frac{\partial T}{\partial x_j}g_j\right), \quad \mu_t = \frac{C_\mu \rho k^2}{\epsilon}$$

$$\sigma_k = 1.0,\ \sigma_h = 0.9,\ \sigma_\epsilon = 1.3,\ C_1 = 1.44,\ C_2 = 1.92,\ C_\mu = 0.09$$

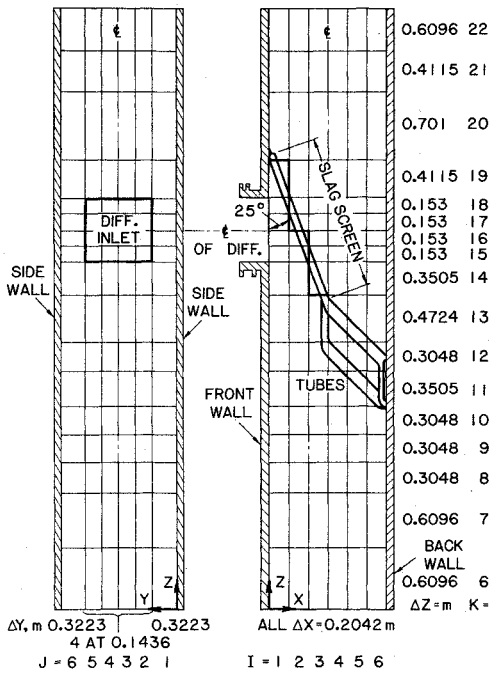

Fig. 1 Front and side views of the CFFF radiant furnace showing coarse mesh nodalization.

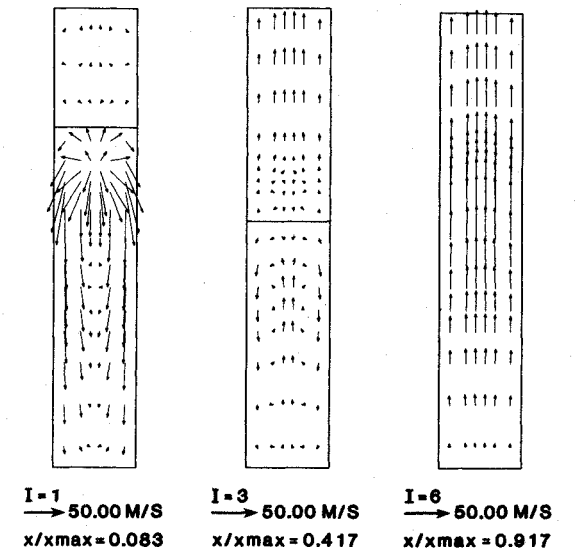

Fig. 2 Velocity vectors in *J-K* planes $I=1$, 3, and 6 (coarse mesh), respectively.

thick, extends at an angle of about 25 deg to the vertical front wall across the entire width of the furnace above the diffuser exit to its center, where it separates into a two-row, staggered tube bank.

COMMIX-1A Geometric Model and Computational Results for Test LMF1C 4-5

Figure 1 presents the coarse mesh nodalization, index notation *I, J,* and *K* in the three directions *x, y,* and *z* superimposed on the simplified front and side views of the CFFF radiant furnace. The furnace cross-section was divided into 6×6 computational nodes. The furnace height was divided into 17 nodes for a total of 612 nodes. The *K*-direction nodalization index begins at $K=6$. The slag screen was approximated as a "zig-zag" (as indicated by the heavy lines on the side view in Fig. 1) with zero flow through its surfaces. The staggered tube bank was modeled as a porous medium with an assumed porosity. The diffuser inlet was divided into 4×4 nodes and extends from $J=2$ to $J=5$ and from $K=15$ to $K=18$ as shown in Fig. 1.

Conditions used for the isothermal simulation were inlet velocity, 60 m/s; velocity profile, uniform; pressure, 1.03×10^5 Pa; density, 0.15 kg/m^3; turbulent viscosity, 0.01 Pa·s; and laminar viscosity, 1.09×10^{-4} Pa·s. The physical properties correspond to air. The turbulent viscosity was estimated from a simple model.[6,10] It is a single constant value that is added to the laminar viscosity throughout the computational region.

The flow patterns in the *J-K* planes $I=1$, 3, and 6 progressing from the diffuser inlet on the front wall to the back wall are shown in Fig. 2. Plots near the front wall indicate that the combustion gases strike the solid slag screen (horizontal solid line), spread as a jet, and flow downward caused by the confinement of the slag screen and the furnace side walls. Flow recirculation is observed below the slag screen for $I=1$ and $I=3$. The recirculation is more pronounced at $I=3$, which is near the center of the furnace. The gases then proceed to flow upward through the staggered tubes at $I=6$.

The velocity vectors in the *I-K* planes $J=4$-6 are shown in Fig. 3. Because of symmetry, *I-K* planes $J=1$-3 are omitted. These plots confirm that the downward flow is strongest near the side wall, $J=6$. The gas turns 180 deg and flows upwards through the staggered tube bank. The velocity vectors crossing the solid slag screen in Fig. 3 do not imply any flow across the slag screen. They merely indicate the relative magnitudes of the velocity vectors.

The velocity vectors in the *I-J* planes $K=10$ and 14 are shown in Fig. 4. Below the solid slag screen at $K=10$ the basic flow is from the front wall to the back wall. Near the bottom of the slag screen (represented by the vertical solid line) at $K=14$, the gas flow is diverted to the side walls. There is a recirculation pattern to the right of the slag screen where flow is primarily upward as shown in Fig. 2. The recirculation pattern becomes stronger as the gas flows upwards.

Sensitivity Analyses

The results of this first calculation reveal complex three-dimensional flow patterns. These flow patterns indicate that a portion of the flow does go towards the bottom of the furnace. They also show recirculation both below and above the slag screen. Additional scoping studies were performed to assess the sensitivity of these flow patterns to changes in the modeling methodologies.

The first variation in the model was to introduce a nonuniform flow entering the furnace through the diffuser inlet. In reality, the flow would never be perfectly uniform entering the furnace. However, there were no measurements made to determine the inlet velocity profile. The central core of the flow entering the furnace was increased to 120 m/s, and the flow in the area surrounding this central core was reduced to 40 m/s while maintaining the same mass flow rate. Calculated results indicate that the flow patterns are similar to those for which uniform inlet flow was assumed. The flow is slightly lower near the side walls. Some changes in the recirculation regions were also observed, but no significant variations either in location or strength could be ascertained. Thus, it is concluded that variations in the inlet velocity distribution are not very important in modeling flows in the radiant furnace since these variations affect only a local region in the vicinity of the slag screen. These variations could be significant in modeling erosion and slag collection efficiency, but that was not the objective of this paper.

The next modification to the model involved a smaller node size. The major reason for doing this was to improve the resolution of the "zig-zag" approximation to the slag screen. The finer mesh model is shown in Fig. 5. The slag screen region was divided into six nodes in the *I*-direction (there were

three nodes in the coarse mesh model). The region containing the staggered tube bank was divided into three nodes as before. The J-direction was modeled with 10 nodes instead of six nodes. In actual computation, only five nodes were needed because of the assumption of symmetry. The total number of nodes amounted to 945, more than three times that of the coarse mesh.

The velocity vector plots computed with the finer mesh are presented in Figs. 6 and 7. Figure 6 shows the calculated flow patterns in three selected J-K planes corresponding closely to those shown in Fig. 2. The axis of symmetry is on the right side of each plot. Except for finer resolution of flow details, the basic flow patterns are the same as for the coarse mesh. The velocity is higher in the vicinity of the slag screen because of the better resolution of the angled slag screen. The downward flow near the side walls at $I=1$ is even higher than the previous results. For example, the maximum downward velocity near the side walls increased from approximately 50 m/s (coarse mesh) to 55 m/s. The recirculation region below the slag screen at $I=6$ was also resolved better. The upward flow at $I=9$ very closely resembles the coarse mesh results.

Three selected velocity vector plots in the I-K planes from $J=1$ to $J=5$ proceeding from near the furnace side wall to near the furnace centerline are shown in Fig. 7. The flow patterns agree closely with those shown in Fig. 3. Even though the finer mesh computation may not be grid independent, it provides a better resolution of major phenomena for subsequent analyses, even though there may be some numerical diffusion effects.

The next variation in the model was to remove the tubes completely. This is equivalent to setting the volume and surface porosities to 1.0. Almost no changes in the velocities were observed. It is concluded that the tube bank could be simply modeled with only rough estimates of porosity.

Next, the problem was run using the so-called two-parameter k-ϵ turbulence model. This model is not in COMMIX-1A, but it is in the COMMIX-1B, which is soon to be released.[13] The model equations and constants are given in Table 1.

The results of the computations for the coarse mesh reveals no significant variations in the flow patterns. This may be due to the fact that the flow is mostly entrance region type. In this case velocity profiles computed with a constant turbulent viscosity or the two-parameter turbulence model agree closely with each other and with experimental data.[13] The velocity profiles exiting at the top of the furnace are flatter. Because the computation time of the two-parameter turbulence model was nearly three times longer than that of the constant turbulent viscosity model, the benefit of a possibly more accurate velocity calculation did not seem justified. One benefit of using the more sophisticated model was that the turbulence kinetic energy, dissipation, and viscosity distributions could be evaluated. The values of the turbulent viscosity computed from the k-ϵ model straddled the estimated constant value of 0.01 Pa·s. In some regions, such as near the slag screen, they were higher; and in some regions, such as in the recirculation regions, they were lower. All further runs were made using a constant value of turbulent viscosity.

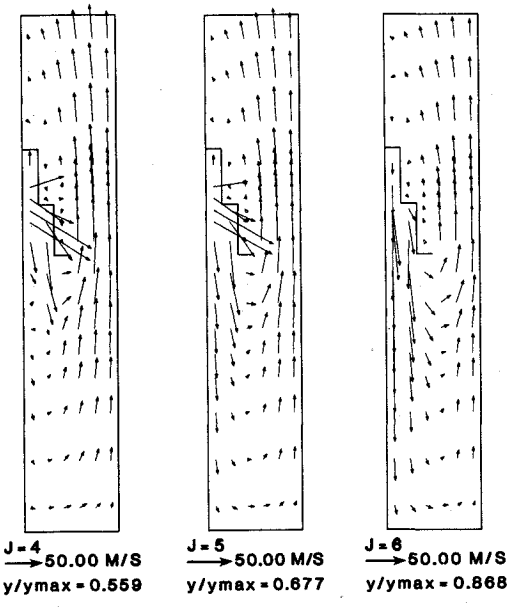

Fig. 3 Velocity vectors in I-K planes $J=4$ through 6 (coarse mesh).

Analysis of UTSI Test LMF1C 4-5

Test LMF1C 4-5 is analyzed in this section both isothermally and nonisothermally. The objectives were to develop some quantitative estimates of both the flow split produced by the slag screen and the temperature and heat flux distribution in the radiant furnace section. Minor variants of the finer mesh model described in the previous section were used.

The inlet conditions for test LMF1C 4-5 are as follows: temperature, 2380 K (2107°C); mass flow rate, 3.64 kg/s; inlet velocity, 65.43 m/s; velocity profile, uniform; and density, 0.158 kg/m^3.

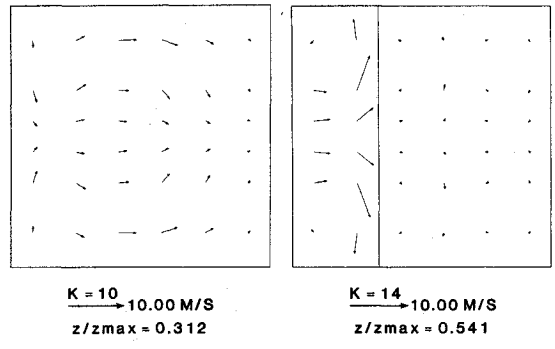

Fig. 4 Velocity vector plots in I-J planes $K=10$ and 20 (coarse mesh).

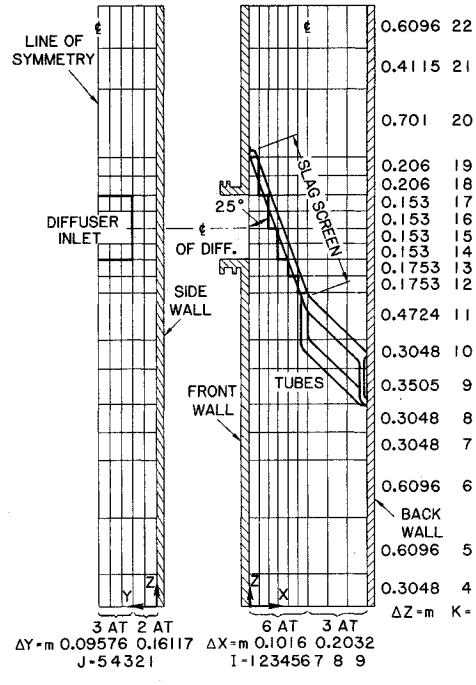

Fig. 5 Front and side views of the CFFF radiant furnace showing finer mesh nodalization.

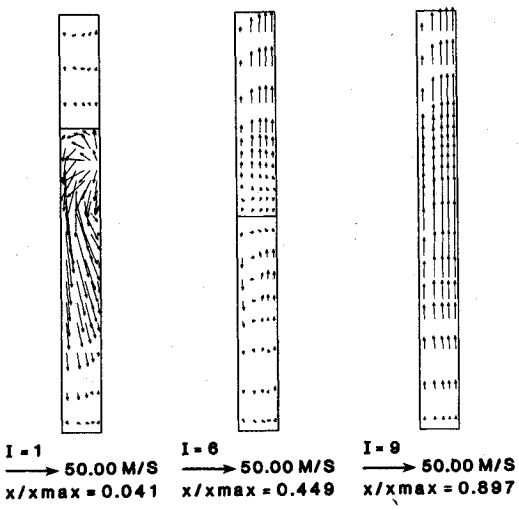

Fig. 6 Velocity vector plots in *J-K* planes $I=1$, 6, and 9 (fine mesh), respectively.

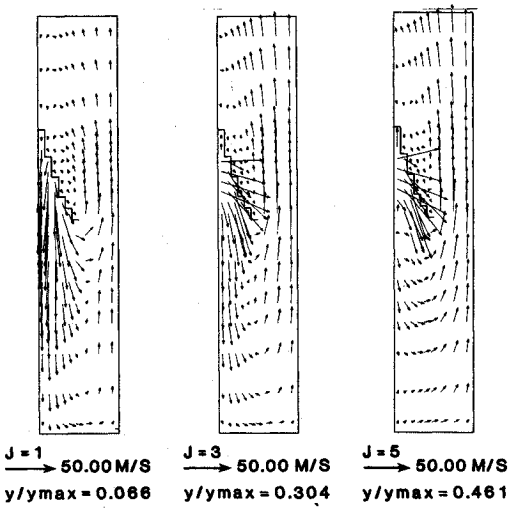

Fig. 7 Velocity vector plots in *I-K* planes $J=1$, 3, and 5 (finer mesh), respectively.

Isothermal Flow Split Analysis

First an isothermal run was performed in order to more easily obtain an estimate of the flow split produced by the slag screen. The computed velocity vector plots closely resemble the finer mesh scoping study results shown in Figs. 6 and 7.

Because of the three-dimensional nature of the flow, the flow split varies from the plane of the inlet as well as along the slag screen. The flow split was computed for the vertical plane right below the end of the slag screen located at the center of the furnace. This plane was divided into two approximately equal portions, the upper half right below the slag screen and the lower half further away from the slag screen. The flow split was computed on the basis of mass fluxes, which in turn can determine the velocity distribution since the density is constant in the computation.

The average velocities int the direction normal to the vertical plane below the slag screen were computed for the upper and lower half planes. The average velocity in the upper half plane near the side wall is significantly higher than the average velocity in the lower half plane near the side wall (8.29 m/s vs 3.41 m/s). The average velocities along the slag screen reveal a tendency for the flow to favor the center and the side walls.

The average velocity of the entire upper half plane (5.72 m/s) is slightly higher than the average velocity of the entire bottom half (5.54 m/s). Since the average velocity for the entire plane is 5.63 m/s, overall the flow can be said to be almost uniform but with a tendency to be slightly higher near the slag screen and near the center of the furnace. Thus, the flow splits into two nearly equal paths.

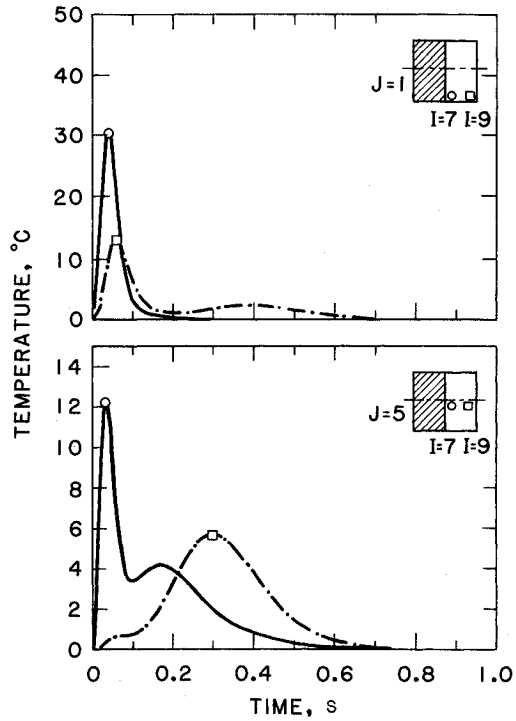

Fig. 8 Thermal tracer curves at $K=11$ for the UTSI CFFF.

Tracer Analysis

A transient three-dimensional tracer computer simulation was performed to gain further insight into the flow patterns of the gas. A tracer study for a fluid system usually involves the introduction of a pulse into the system. The pulse introduced should be detectable and should not significantly affect the flowfield. Analysis of the tracer response to the fluid flow yields information about the extent of mixing in the system.[14]

In this computer study, a thermal tracer was used. The flowfield used is the same one analyzed in the previous section. This flowfield was held constant and used as input to the tracer calculation, and the furnace walls and the slag screen were assumed adiabatic. An initial ambient temperature of 273 K was assumed for the entire flow, except for a plane pulse of heated gas at 1273 K introduced across the diffuser inlet. The temperature entering the diffuser inlet was maintained at 273 K. The tracer study contained herein determined the approximate response times of the peak temperatures at various key locations in the radiant furnace.

The thermal response curves in the region at the bottom and to the right of the slag screen at axial plane $K=11$ shown in Fig. 5 are presented in Fig. 8. The response near the slag screen and near the side wall (the circle at $I=7$, $J=1$ in the inset) is sharp and peaks at about 0.04 s. The response near the back wall (the square at $I=9$, $J=1$ in the inset) is less sharp, peaking at 0.06 s. A second broader response peaks at about 0.4 s. Near the furnace center and near the slag screen ($I=7$, $J=5$), the thermal response has a sharp peak first at about 0.04 s and a weaker second peak at about 0.18 s with a rather slow decay and long "tail." The strength of the first peak near the furnace center near the slag screen is weaker than near the side wall, indicating more mixing has occurred. The response near the back wall ($I=9$, $J=5$) reaches a plateau at about 0.05 s and then peaks again at about 0.3 s.

Examination of these thermal response curves together with the velocity plots, such as those shown in Fig. 7, strongly rein-

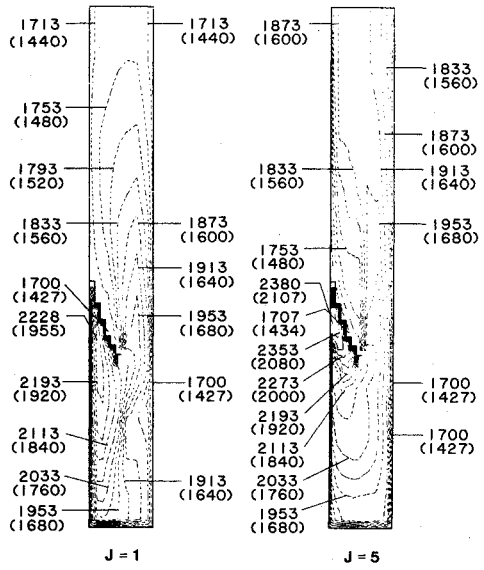

Fig. 9 Isotherm plots in *I-K* planes $J=1$ and 5. Temperatures are in K(°C).

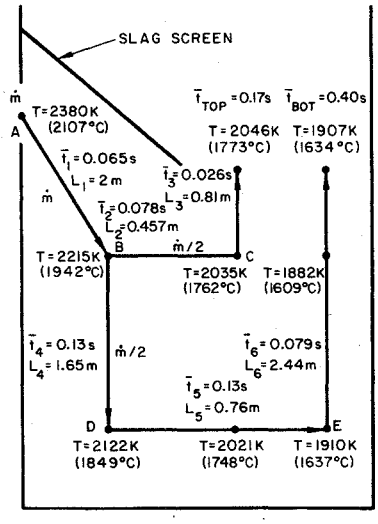

Fig. 10 Simplified parallel-path temperature/flow model of the UTSI CFFF radiant furnace.

forces the explanation of the gas flow patterns and their effects on the mixing process. Clearly, there are two distinct flow paths, one close to the slag screen and the other further below it. The manner in which these flow paths rejoin varies from the side wall to the center of the furnace. The double-peaked response curves indicate two parallel flow channels.

The double-peaked responses (such as at the back wall, shown in Fig. 8 at $I=9$, $J=1$) can be considered as a superposition of two response curves, one originating from flow near the slag screen and the other one from further down below the slag screen. These flow patterns can be observed also in Fig. 7 at $J=1$. The times that the peaks occur are roughly the residence times of these flow paths. There is only a single peak near the end of the slag screen, because the strong flow there deflects the flow rising from the bottom toward the back wall.

The double-peaked response in Fig. 8 at $I=7$, $J=5$ and $I=9$, $J=5$ are caused by the flow split at the solid screen. The flow path accounting for the second response near the back wall is longer than the second response near the slag screen. The long "tails" in both curves indicate that recirculation exists, trapping a portion of the warm fluid and delaying complete fluid mixing.

The heights and widths of the response curves indicate the degree of mixing and, therefore, the extent of dispersion. These observations have been used to develop a one-dimensional representation of the three-dimensional flow and temperature calculations, which will be described later.

Heat Transfer Analysis

In this section, the steady-state coupled flow and heat transfer analysis of Test LMF1C 4-5 is described. COMMIX-1A does not yet have a radiation heat transfer model. The radiation component of heat transfer has been simulated by adding a constant to the Nusselt number correlation for turbulent convection over a flat plate.[15] In order to estimate this constant, which can be considered the result of linearizing T^4 radiation, the heat transfer results from using the KINE code (which does have a T^4 radiation model) have been used. The results indicate that about 85% of the total heat transfer is by radiation. Using an average Prandtl number of 0.63 for air, the model developed was

$$Nu = 3500 + 0.03(Re)^{0.8} \tag{2}$$

where Nu and Re are the Nusselt and Reynolds numbers, respectively. Equation (2) simulates and 85% radiative component at a gas velocity of 30 m/s.

Calculations were performed for the primary furnace that contains the slag screen and up to 4 m above the primary furnace. All of the furnace walls and the slag screen were assumed to be covered with a molten slag layer having a constant temperature of 1700 K. This was modeled by fixing the wall temperatures at this value and computing the heat flux to the gas using Eq. (2). Heat transfer to the staggered tube bank modeled as a porous medium was assumed to be about 2.5% (1.5×10^5 W) of the total heat removed from the furnace.[2] This was modeled by specifying a volumetric heat sink of 2.1×10^5 W/m^3 and a tube bank volume porosity of 0.5. The computed gas temperature at 4 m above the primary furnace was 1850 K (1577°C), which compares favorably with the one-dimensional temperatures computed by ANL and UTSI, respectively, at the same location.

Because the buoyancy effect was not significant, the velocity field computed with heat transfer was almost identical to the velocity field computed isothermally. The velocity vector plots are similar to those shown in Figs. 6 and 7. The gas temperatures indicated by isotherms in the *I-K* planes $J=1$ and $J=5$ are shown in Fig. 9 near the side wall and the centerline of the furnace. Below the slag screen, the computed gas temperatures were highly nonuniform, so the assumption of a one-dimensional well-mixed model below the slag screen is not appropriate. Well above the screen, gas temperatures are essentially uniform. The temperatures are higher below the slag screen near the side wall than near the centerline, while the temperatures above the slag screen are lower. The low temperatures in the recirculation region above the slag screen are clear.

The wall heat transfer rates and the average wall heat fluxes to the radiant furnace were analyzed. The average heat fluxes to the front, back, and two side walls are fairly uniform at $2.1\text{-}2.7\times10^4$ W/m^2. The heat flux to the bottom is somewhat higher because the projected area instead of the actual surface area of the bottom was used in the calculations. The heat flux to the slag screen is highest at about 12×10^4 W/m^2. The calculated total heat removed by the furnace up to 4 m above the primary furnace and including the slag screen and the staggered tubes is about 2 MW.

Simplified Temperature/Flow Model for the CFFF Radiant Furnace and Nitric Oxide Decomposition Calculations

The three-dimensional flow, tracer, and heat transfer analyses described earlier were combined to develop an

idealized and simplified temperature/flow model to analyze experimental NO decomposition data using a one-dimensional chemical kinetics code. This model, although idealized, is believed to represent realistic estimates of the basic flow patterns and temperatures in the CFFF radiant furnace with a slag screen.

Simplified Temperature/Flow Model

The model is illustrated in Fig. 10. The region below the slag screen was divided into two approximately equal top and bottom sections. Results from the flow split study indicate that the average gas flows crossing the vertical plane of the furnace are about the same in the top and bottom sections below the slag screen. Thus, the inlet gas flow of $\dot{m}$ at point A was assumed to travel along path L_1 to point B, located at the centerline of the top section, and to split into two equal portions (each $\dot{m}/2$). The first portion of the gas travels along the path L_2 to point C, one-fourth of the way from the furnace center; the gas then travels upward along path L_3. The other portion of the gas travels downward along path L_4 from point B to point D, located at the centerline of the bottom section; gas then flows horizontally along path L_5 to E, three-fourths of the way from the furnace center, then flows upward along path L_6. The temperatures indicated in Fig. 10 are the average values of the temperatures computed by COMMIX-1A for all five J-planes at these points.

The total estimated residence times $\bar{t}_{TOP}$ and $\bar{t}_{BOT}$ which are the sums of the individual estimated residence times $\bar{t}_1$-$\bar{t}_6$, shown in Fig. 10 for the shorter and the longer flow paths, are 0.17 and 0.40 s, respectively. These residence times are approximately the same as the average times of the double-peaked responses found in the tracer analysis.

Nitric Oxide Decomposition Computations

At ANL, a one-dimensional chemical kinetics code KINE[4] was developed to calculate the gas compositions (including NO) in high-temperature gas ducts, such as radiant boilers. Formulation of the NO reactions in this code began with the following equations:

$$N_2 + O = NO + N \quad (3)$$

$$NO + O = N + O_2 \quad (4)$$

and

$$NO + H = OH + N \quad (5)$$

Equations (4) and (5), together with $O_2 - O$ equilibrium reaction

$$O_2 + M = 2O + M \quad (6)$$

(where M is a third-body term), have been widely used in calculating NO concentrations at high temperatures. Equation (3) is significant under reducing conditions. These four reactions form the basis of the code. Other reactions include the O_2/H_2 and the carbon reactions. The O_2/H_2 reactions, involving O_2, OH, and H, would influence the three NO reactions. The carbon-compound reactions were included because of the interaction of hydrogen and oxygen with the carbon compounds. Reactions involving sulfur were not included. The 30 reactions involving the elementary reactions involving the nitrogen, oxygen and hydrogen species, the value of the Arrhenius reaction rate constants and the corresponding third-body efficiencies are listed in Tables 1 and 2 of Ref. 16.

Predictions using this code have been verified to some degree with experimental data.[17] In one option of this code, the initial gas composition and gas flow and the gas temperatures along the length of the furnace are specified; the gas compositions along the duct are computed. In another option, the chemical kinetics calculations are coupled with a model of radiant and convective heat transfer. In this option,

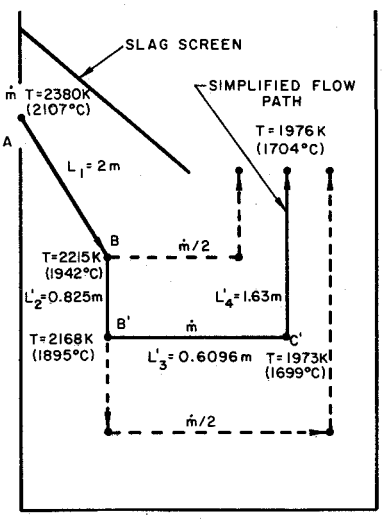

Fig. 11 Simplified one-dimensional temperature/flow model of the UTSI CFFF radiant furnace.

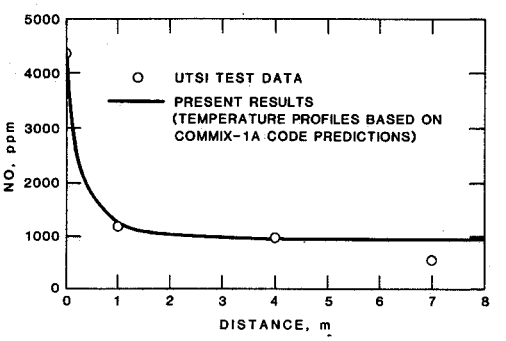

Fig. 12 Measured and predicted NO concentrations for test LMFIC 4-5.

the initial gas compositions, gas temperature, and gas flow are specified; the gas compositions and temperature along the duct are computed. Nitric oxide calculations presented in this paper were performed using the first option. For this reason the results shown in Fig. 10 were simplified even further to a single equivalent length model, as shown in Fig. 11. All of the gas was assumed to flow downward from point B along path L_2 to the middle of the furnace below the slag screen to point B'. The gas proceeds horizontally along path L_3' until reaching a distance of one-fourth of the furnace width away from the furnace center at point C', and then flows upwards. The total length of the equivalent flow path is approximately 5.1 m. This simplified one-dimensional temperature/flow model was used in the KINE code to calculate the NO concentrations shown in Fig. 12. As can be seen, the results are in good agreement with the data.

Conclusions

Based on the analyses performed in the paper, we have arrived at the following major conclusions:

1) A general methodology has been developed which produces a simplified one-dimensional representation of the three-dimensional flow and temperature calculations for use in a one-dimensional chemical kinetics code.

2) The analyses of the NO data from the LMF1C test series at the UTSI CFFF demonstrate that, in addition to using a chemical kinetics code, an understanding of the temperature and flow profiles of the combustion gases is essential in comparing calculated NO concentrations with the experimental data.

3) The isothermal, nonisothermal, and tracer analyses indicate that the fluid flow and temperature distributions in the UTSI radiant furnace, with a slag screen, are highly three-dimensional.

4) The methodology developed does an adequate job in analyzing the UTSI NO decomposition data. However, future studies should be directed toward developing a three-dimensional chemical kinetics code that can use the results of a three-dimensional thermal hydraulics code, to provide straightforward calculations rather than having to simplify the calculations to a one-dimensional representation.

Acknowledgments

The authors wish to acknowledge the use of the test data from the University of Tennessee Space Institute and the numerous discussions with Lloyd Crawford, James Chapman, Richard Attig, Norman Johanson, and Susan Wu on the modeling of NO decomposition predictions in an MHD radiant furnace.

References

[1]Shaver, T. C. and White, M. K., "Ash Deposition, Metal Corrosion, and Refractory Performance in a Coal-fired MHD Test Train," *Proceedings of the 21st Symposium on Engineering Aspects of Magnetohydrodynamics,* Argonne National Laboratory, Argonne, IL, June 1983, pp. 8.5.1-8.5.12.

[2]Lineberry, J. T., Galanga, F. L., and Gonzalez, D. E., "Gas Dynamic and Heat Transfer Evaluation of the CFFF LMF1 Flow Train," *Proceedings of the 21st Symposium on Engineering Aspects of Magnetohydrodynamics,* Argonne National Laboratory, Argonne, IL, June 1983, pp. 2.5.2-2.5.18.

[3]Crawford, L. W., Attig, R. C., Chapman, J. N., and Lynch, T. P., "Nitrogen Oxide Control in a Coal-Fired MHD System," *Proceedings of the 21st Symposium on Engineering Aspects of Magnetohydrodynamics,* Argonne National Laboratory, Argonne, IL, June 1983.

[4]Sistino, A. J., "Analytical Studies of NO_x Decomposition in the Radiant Boiler of an Open Cycle MHD Power Plant," Argonne National Laboratory, Argonne, IL, ANL/MHD-79-7, April 1979.

[5]Sacks, R. A., Geyer, H. K., Grammel, S. J., and Doss, E. D., "Modified NASA-Lewis Chemical Equilibrium Code for MHD Applications," Argonne National Laboratory, Argonne, IL, ANL/MHD-79-15, Dec. 1979.

[6]Domanus, H. M., Schmitt, R. C., Sha, W. T., and Shah, V. L., "COMMIX-1A: A Three-Dimensional Transient Single-Phase Computer Program for Thermal Hydraulic Analysis of Single and Multicomponent Systems, Volume I: Users Manual," Argonne National Laboratory, Argonne, IL, ANL-82-25, Vol. I, NUREG/CR-2896, Vol. I, Dec. 1983.

[7]Domanus, H. M., Schmitt, R. C., Sha, W. T., and Shah, V. L., "COMMIX-1A: A Three-Dimensional Transient Single-Phase Computer Program for Thermal Hydraulic Analysis of Single and Multicomponent Systems, Volume II: Assessment and Validation," Argonne National Laboratory, Argonne, IL, ANL-82-25, Vol. II, NUREG/CR-2896, Vol. II, Dec. 1983.

[8]Lyczkowski, R. W., Fuhs, H. P., Baumann, W. L., Domanus, H. M., and Sha, W. T., "Analysis of OCONEE Unit-1 Downcomer and Lower Plenum Thermal-Mixing Tests Using COMMIX-1A," Final Rept. for Research Project 1749-2, Electric Power Research Institute, Palo Alto, CA, EPRI NP-3780, Nov. 1984.

[9]Lyczkowski, Miao, C. C., Domanus, H. M., Hull, J. R., Sha, W. T., and Schmitt, R. C., "Three-Dimensional Analysis of Thermal and Fluid Mixing in Cold Leg and Downcomer of PWR Geometries," Interim Rept. Research Project 2122-1, Electric Power Research Institute, Palo Alto, CA, EPRI NP-3321, Dec. 1983.

[10]Sha, W. T., Domanus, H. M., Schmidt, R. C., Oras, J. J., and Lin, E. I. H., "COMMIX-1: A Three-Dimensional Transient Single-Phase Component Computer Program for Thermal-Hydraulic Analysis," Argonne National Laboratory, Argonne, IL, ANL-77-96, NUREG/CR-0785, Sept. 1978.

[11]Harlow, F. H. and Amsden, A. A., "A Numerical Fluid Dynamics Calculation Method for All Flow Speeds," *Journal of Computational Physics,* Vol. 8, 1971, pp. 197-213.

[12]Domanus, H. M., Schmitt, R. C., Sha, W. T., and Shah, V. L., "A New Implicit Numerical Scheme in the COMMIX-1A Computer Program," Argonne National Laboratory, Argonne, IL, ANL-83-64, NUREG/CR-3435, Sept. 1983.

[13]Chen, F. F., Domanus, H. M., Sha, W. T., and Shah, V. L., "Turbulence Modeling in the COMMIX Computer Code," Argonne National Laboratory, Argonne, IL, ANL-83-65, NUREG/CR-3504, EPRI NP-3546, April 1984.

[14]Lyczkowski, R. W., Thorsness, C. B., and Cena, R. J., "The Use of Tracers in Laboratory and Field Tests of Underground Coal Gasification and Oil Shale Retorting," *Proceedings of the 4th Underground Coal Conversion Symposium,* Steamboat Springs, CO, June 1978, pp. 239-256.

[15]Knudsen, J. G. and Katz, D. L., *Fluid Dynamics and Heat Transfer,* McGraw-Hill, NY, 1958, p. 488.

[16]Chow, L. S. H., Wang, C. S., Lyczkowski, R. W., Johnson, T. R., and Berry, G. F., "Analysis of the CFFF Nitric Oxide Data," Argonne National Laboratory, Argonne, IL, ANL/MHD-84-4, Dec. 1984.

[17]Sistino, A. J., "Comparison of Analytical and Experimental Studies of NO_x Kinetics in MHD Systems," Argonne National Laboratory, Argonne, IL, ANL/MHD-80-17, Feb. 1981.